Preparation of Anthryl Group-Tagged Helical Poly(γ-benzyl L-glutamate) Self-Assembled Film on Gold Surface and Its Interaction with DNA

Masazo Niwa,* Masa-aki Morikawa, Tomohiro Nabeta, and Nobuyuki Higashi*

Department of Molecular Science & Technology, Faculty of Engineering, Doshisha University, Kyotanabe, Kyoto 610-0321, Japan

Received September 10, 2001; Revised Manuscript Received December 18, 2001

ABSTRACT: A novel poly(γ-benzyl-L-glutamate) (PBLG, **1**), which has an anthryl group at the C-terminus of PBLG segment, has been synthesized, and its immobilization onto gold surface based on a specific interhelix interaction and DNA binding property at a self-assembled monolayer surface have been studied. A PBLG carrying a S−S bond at the C-terminus, **3**, formed self-assembled monolayers on a gold surface. Within a resulting monolayer of **3**, helical rods of the PBLG segment were oriented in the antiparallel manner, allowing an attractive interaction between helix macrodipoles. When a helix-breaking solvent such as DMSO was added to the solution, about a half amount of the adsorbate was released from the monolayer, followed by weakening the interhelix interaction, and a porous monolayer including molecular cavities was formed. Such a cavity size should fit the occupied volume of the helices present in the original assembly. Guest helices of **1** and **2**, which has a similar molecular structure to that of **1** except for the lack of the anthryl moiety, could interact with the host porous monolayer of **1** on gold substrates. The binding properties of DNA onto **1**, **2**, and **3** mixed monolayers, in which anthryl groups must be located at the monolayer surface, were examined by means of quartz crystal microbalance and X-ray photoelectron spectroscopy. The results indicated that DNA bound to the PBLG mixed monolayers when the anthryl groups at the monolayer surface were in an optimized distribution.

Introduction

A great deal of research interest has been focused on the construction of organized polypeptide monolayer on a solid support by the self-assembling technique.[1−4] To reveal the self-organization mechanism of polypeptides must be a key element for developing high performed, peptide-based materials, since protein functions would derive from such highly organized structures. In this context, we have devised a strategy in which a purely synthetic polypeptide such as poly(L-glutamic acid) is aligned on two-dimensional media.[5−9] In our recent work, it has been found that a self-assembled monolayer (SAM) of poly(L-glutamic acid) carrying an S−S bond at the N-terminus has the ability to discriminate between N- and C-termini of guest polypeptides in water on the basis of helix−macrodipole interactions.[6] In addition, the spontaneous formation of a double-layered poly(γ-benzyl-L-glutamate) (PBLG) having an S−S bond at the chain end on gold surface has been observed, and such a unique structure was rationalized in terms of an antiparallel association property of helical rods, allowing an attractive interaction between macrodipoles.[10]

SAMs of *n*-alkanethiols deposited on gold have been widely studied and used for a range of applications because of their powerful potentials and ease to fabricate highly ordered, stable structures.[11−15] Functionalized monolayers assembled onto gold surfaces are currently examined as sensor interfaces[16] and active surfaces for patterning[17] and chemical architecture[18] of solid supports. The construction of supramolecular systems at surfaces, where various functional groups are tagged at a proposed position, must result in an intelligent molecular-scale device. Recently, we have demonstrated that the successful immobilization of DNA is accomplished onto a cationic SAM film on gold surface on the basis of the electrostatic interaction[19] and onto the acridine-tethered SAM film through intercalation.[20] In this paper, we propose a new approach to immobilization of such functional groups at the monolayer surface by using helix−macrodipole interaction.

The DNA−protein hybridized structure is interested not only in the biological information but also in molecular materials such as electron conducting media[21−23] since the DNA itself has π-electron clouds of stacked base, and the helical polypeptide generates the electrostatic potential directed from the N-terminus to the C-terminus by a macrodipole.[24,25] Thus, if the helical polypeptide assemblies are hybridized with DNAs, it is expected that novel functions such as the current rectified molecular wire would be realized. We describe herein the organization of "peptide intercalator", which has a DNA intercalatable moiety at one terminal end of the polypeptide segment, by incorporating into the polypeptide underlayer through a specific interhelix interaction and then the binding property of DNA onto this intercalator-tethered peptide film. The stepwise preparation of anthryl group-tagged helical peptide self-assemblies and their interaction with DNA is schematically represented in Chart 1. PBLGs with and without anthryl group at the C-terminus of PBLG segment **1** and **2**, respectively, are newly prepared and used as guest peptide intercalators. PBLG having an S−S bond at the C-terminus, **3**, is also synthesized and used as a monolayer former on a gold surface.

Experimental Section

Materials. PBLG having an anthryl group and an S−S bond at the C-terminus **1** and **3**, respectively, and the control compound, **2**, were synthesized as follows. The products were identified by visible, IR, and ^{1}H NMR spectoscopies, and their

10.1021/ma0116093 CCC: $22.00 © 2002 American Chemical Society
Published on Web 02/16/2002

Chart 1

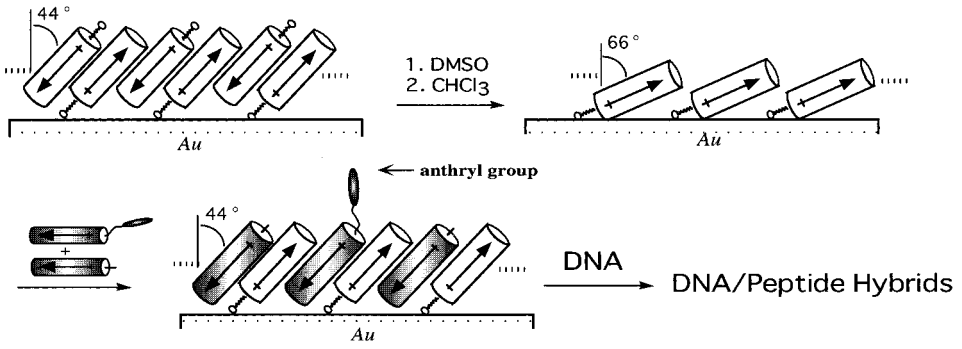

Chart 2

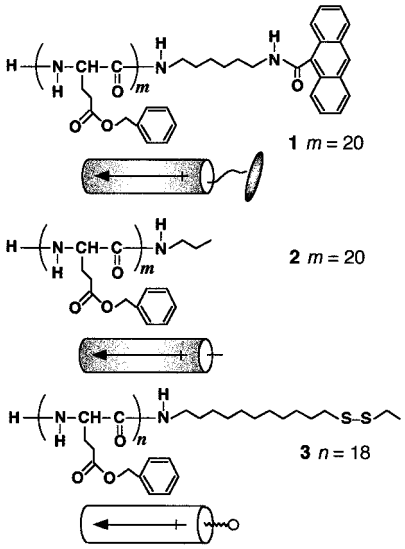

Scheme 1

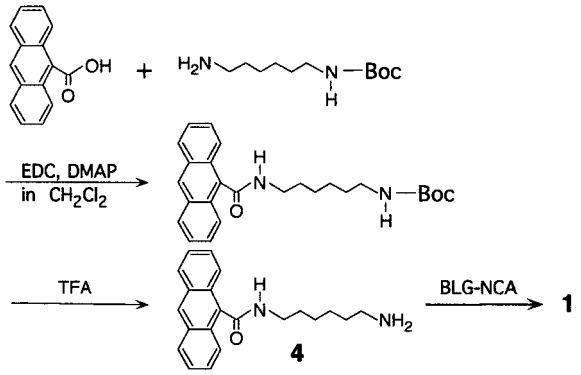

Scheme 2

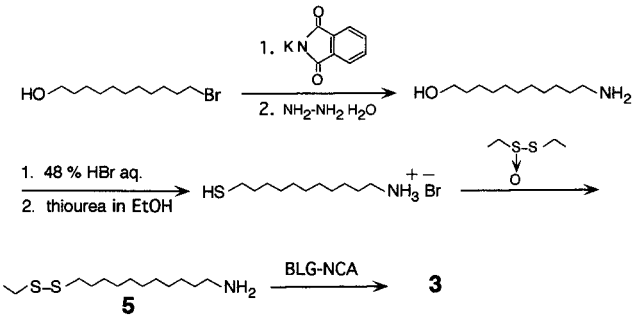

purity and molecular weight distribution (MWD) were checked by thin-layer chromatography (TLC) and matrix-assisted laser desorption ionization time-of-flight (MALDI-TOF) mass spectrometry, respectively.

PBLG (1). Anthracene-9-carboxylic acid was dissolved in CH_2Cl_2 and was reacted with *N*-(*tert*-butoxycarbonyl)-1,6-diaminohexane in the presence of 1-ethyl-3-(3-(dimethylamino)propyl)carbodiimide hydrochloride with 4-(dimethylamino)pyridine at room temperature for 24 h. After removal of CH_2Cl_2, the residue was purified by recrystallization from THF to give a pale-yellow solid and was added to trifluoroacetic acid. The solution was stirred at room temperature for 2 h, and trifluoroacetic acid was then removed. The crude product was washed with 0.1 M potassium carbonate aqueous solution several times and dried. *N*-(Anthracene-9-carbonyl)hexanediamine (**4**) thus obtained was immediately used as an initiator for the polymerization of γ-benzyl-L-glutamate−*N*-carboxylic anhydride (BLG−NCA) in $CHCl_3$. After removal of $CHCl_3$, the residue was purified by washing with diethyl ether several times and dried to give the desired compound, **1**.

PBLG (2). *n*-Propylamine was used as an initiator for the polymerization of BLG−NCA in $CHCl_3$ to give the control compound, **2**.

PBLG (3). 11-Bromo-1-undecanol and phthalimide potassium salt were dissolved in DMF, the mixture was stirred at 50 °C for 6 h, and the insoluble potassium bromide formed was then filtered off. After removal of DMF, the residue was washed with 0.2 M KOH aqueous solution several times and dried to give a white powder. 11-Phthalimido-1-undecanol thus obtained and hydrazine monohydrate were dissolved in ethanol, and the solution was refluxed for 2 h. The resulting precipitate was filtered off, and the solvent was then removed under reduced pressure. The residue was washed with 2 M KOH aqueous solution and water several times and was then added to 48% hydrobromic acid. The solution was stirred at 100 °C for 16 h, and the resulting precipitate at room temperature was recrystallized from acetone to give a pale-brown solid. 11-Bromo-1-undecylamine hydrobromide thus obtained and thiourea were dissolved in ethanol, and the solution was refluxed for 8 h. Hydrolysis of reaction product was then performed, and the corresponding thiol derivative formed was reacted with ethylethanethiosulfinate to give the desired disulfide group-terminated primary amine derivative. 11-(Ethyldithio)-1-undecylamine (**5**) thus obtained was immediately used as an initiator for the polymerization described above, and the desired compound, **3**, was obtained.

The M_w/M_n values, which denote the MWD of these PBLGs, evaluated by MALDI-TOF mass spectroscopy were reasonably narrow (M_w/M_n = 1.07, 1.06, and 1.08 for **1**, **2**, and **3**, respectively).

Preparation of Gold Substrates. A gold disk electrode (BAS, surface area 0.02 cm^{-2}) was cleaned by sonication in 0.1 M KOH aqueous solution for a few minutes and careful polish with diamond and alumina paste (particle size 1 and 0.05 mm, respectively) and then rinsed with water (purified with a Milli-Q purification system, Millipore). A gold-coated electrode for quartz crystal microbarance (QCM) measurement was cleaned by rinsing with $CHCl_3$ and Milli-Q water, respectively, until a frequency change in dry air was not found and then immediately used. Gold substrates on clean glass plates used for reflection−absorption FT-IR and X-ray photoelectron spectroscopy (XPS) measurement were prepared by thermal

evaporation of gold at the pressure of about 10^{-6} Torr and cleaned by rinsing with $CHCl_3$ prior to use.

Measurements. Cyclic voltammetry (CV) was performed at 25 °C with a CV-1B cyclic voltammograph (BAS) connected with an RW-21 *X*−*Y* recorder (Rikadenki, Tokyo). A standard three-electrode configuration was used with the monolayer sample on gold as the working electrode, Ag/AgCl (3 M NaCl) as the reference electrode, and a platinum wire as the counter electrode in a glass vessel. $K_4[Fe(CN)_6]$ was obtained commercially and used as the redox probe in the blocking experiment. The electrolyte solution containing 1 M KCl as a supporting electrolyte were deoxgeneted by purging with nitrogen. The scan rate was kept constant at 100 mV/s for all measurements.

Quartz crystal microbalance (QCM) measurements were performed with gold-coated 9 MHz, AT-cut quartz crystals (USI System, Fukuoka), in which only one side of the resonator was in contact with the surface of the solution. The frequency shifts were recorded continuously with a universal counter (HP53131A, Hewlett-Packard Co., Ltd.) at 20 °C.

Reflection−absorption Fourier transform infrared (RA-FTIR) spectroscopy was performed on a Nicolet System 800 spectrometer with an mercury−cadmium−tellurium (MCT) detector. The measurements were carried out with the 1024 scans of interferogram accumulations using a bare gold substrate as a reference. The optical path was purged with dry air before and during measurements. A reflection attachment at an incident angle of 80° was used together with a polarizer.

X-ray photoelectron spectroscopy (XPS) was performed on a Shimadzu ESCA-1000 system using a Mg Kα source. The takeoff angle of photoemitted electron was set at 90° from the surface. The peak locations were corrected on the basis of the C_{1s} line emitted from neutral hydrocarbon.

Visible absorption spectra were recorded on a Shimadzu UV-2100 spectrometer, using 1 cm path length quartz cells at room temperature. Fluorescence studies were conducted on a Jasco FP-770 spectrofluorophotometer, using 1 cm path length quartz cells at room temperature.

Results and Discussion

DNA Binding Properties of 1 in Solutions. To elucidate the DNA intercalation behavior of **1**, which has an anthryl group at the C-terminus of PBLG segment, the binding experiment was performed in an aqueous solution. Unfortunately, **1** did not dissolve in water, and therefore the benzyl groups were removed to give a water-soluble form **1**(PLGA). The binding experiment was carried out by first dissolving **1**(PLGA) in DMSO and then mixing with calf thymus DNA in an aqueous buffer (50 mM HEPES; buffer/DMSO = 95/5 v/v) at pH 7.2, and the binding process was monitored by means of visible absorption spectroscopy. Figure 1A shows the spectral change of **1**(PLGA) by addition of DNA at various molar ratios of **1**(PLGA) against the phosphate unit of DNA.

The spectra exhibit remarkable hypochromism and a slight red shift of absorption maxima. These observations are explained by a stacking interaction of the intercalated anthryl moiety of **1**(PLGA) with nucleic acid base pairs in DNA without electrostatic contributions.[26−29] The fluorescence studies were also carried out to clarify the intercalation of **1**(PLGA) with DNA. Figure 1B shows the fluorescence emission spectra of **1**(PLGA) in the presence and absence of DNA at various molar ratios in buffer solutions. The addition of DNA led to a drastic fluorescence decrease due to quenching derived from the formation of an anthracene−nucleic acid base complex.[26−29] When the molar ratio of **1**(PLGA) against DNA phosphate unit reaches to be about 50, further spectral changes are not observed in both the absorption and fluorescence spectra. These spectral variation implies that **1**(PLGA) surely works as an intercalator to DNA despite the attachment of a sterically large PLGA segment to the anthryl group.

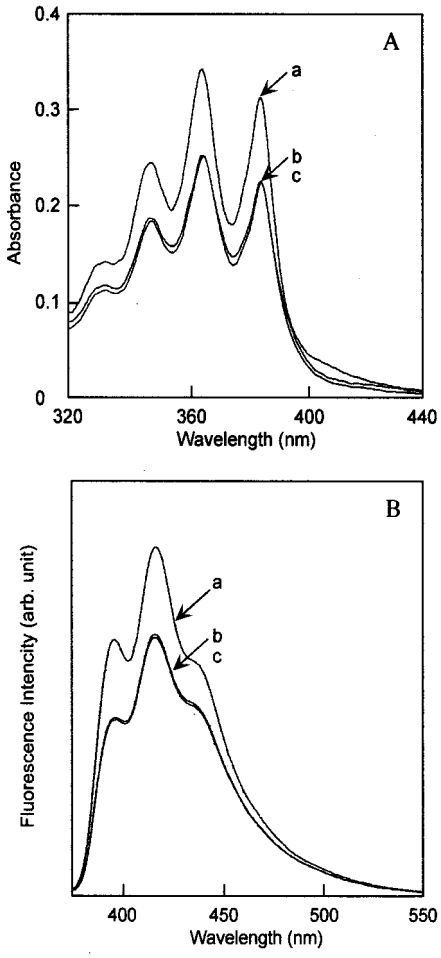

Figure 1. (A) Absorption spectra of **1**(PLGA) in 50 mM HEPES buffer/DMSO (95/5, v/v) at pH 7.2. The concentration of **1**(PLGA) is kept constant at 24 mM, and the concentration of calf thymus DNA is 0 unit M (a), 1.2 unit mM (b), and 1.4 unit mM (c). (B) Fluorescence emission spectra of **1**(PLGA) in 50 mM HEPES buffer/DMSO (95/5, v/v) at pH 7.2 with excitation at 350 nm. The concentration of **1**(PLGA) is kept constant at 5.0 mM, and the concentration of calf thymus DNA is 0 unit M (a), 2.2×10^{-4} unit M (b), and 2.7×10^{-4} unit M (c).

Preparation of Host PBLG Monolayer of 3 on Gold Substrates. The adsorption behavior of **3** onto gold electrode was first examined by means of two independent methods. One of them is the previously established electrochemical method,[30] in which $[Fe(CN)_6]^{4-}$ has been used as a redox couple probing the blocking ability due to adsorption of **3** onto gold surface. Another is to use a quartz crystal microbalance (QCM) that can monitor in situ the adsorption process of **3**, allowing the quantitative estimation of mass increase on gold at nanogram level. Figure 2 shows the change in the anodic peak current (i_{pa}) of $[Fe(CN)_6]^{4-}$ by immersing the gold electrode into $CHCl_3$ solution of **3** at a concentration of 1 mM.

Upon immersion, the peak current apparently decreases and the separation of oxidative and reductive peak potentials increases, indicating that contact of $[Fe(CN)_6]^{4-}$ with electrode surface is depressed due to the adsorption of **3** onto gold surface. Two minutes

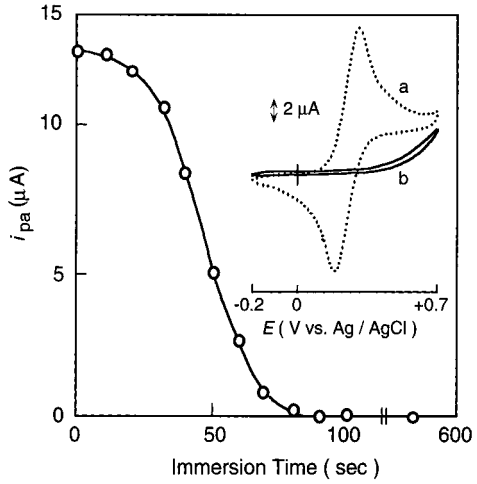

Figure 2. Change in the peak current (i_p) of $[Fe(CN)_6]^{4-}$ due to adsorption of **3** onto gold electrode from $CHCl_3$ solution. Inset shows the typical change in cyclic voltammogram by immersing clean gold electrode into $CHCl_3$ solution of **3**: (a) bare electrode; (b) 90 s immersion. The electrolyte solution is 1 M KCl containing 3 mM $[Fe(CN)_6]^{4-}$.

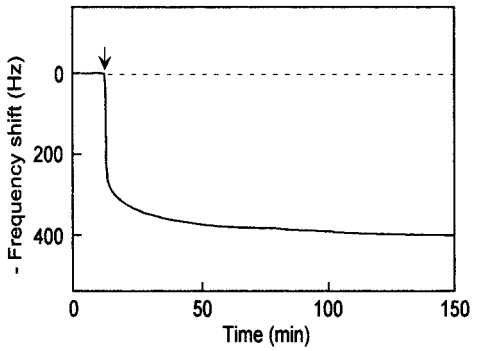

Figure 3. Frequency shift of clean gold-deposited QCM by addition of $CHCl_3$ solution of **3** at the concentration of 8.3 mM.

immersion is found to provide the perfect blocking against $[Fe(CN)_6]$,$^{4-}$ resulting from the formation of a densely packed monolayer of **3** on the electrode. To further confirm the formation of self-assembly of **3** on gold, a QCM technique was also employed. A gold-deposited QCM resonator was placed in pure $CHCl_3$, and the solution of **3** was then added (Figure 3).

The frequency is found to decrease steeply with addition and then becomes unchanged after 2 h at a frequency shift (ΔF) of -44 ± 1 Hz in dry air. The ΔF value can be converted to the mass (Δm) adsorbed on gold surface by Sauerbrey's equation.[31] As a result, Δm value is calculated to be $(2.4 \pm 0.1) \times 10^{-7}$ g/cm^2, and the apparent occupied area of **3** molecule on gold surface can be evaluated to be 2.9 ± 0.1 nm^2 per molecule. This value is well consistent with the cross-sectional area of helical PBLG (2.0−5.3 nm^2),[32] suggesting the formation of a densely packed α-helix assembly of **3** on gold surface. In fact, when the secondary structure of PBLG segment on gold surface was examined by means of FTIR spectroscopy, amide I and II bands were observed at 1655 and 1549 cm^{-1}, respectively, which are characteristic absorptions based on an α-helix structure.[30] In our previous work, it was discovered that helical PBLG existed mainly in a dimeric aggregate in $CHCl_3$.[10] Therefore, the self-assembly of **3** on gold thus obtained would take a double-layered structure consisting of the dimeric aggregate of helices (Chart 1). Such a helix dimer formation must be due to helix−macrodipole interaction and eventually be in side-by-side, antiparallel orientation. The changes both in the blocking ability toward $[Fe(CN)_6]^{4-}$ and in the mass on gold by addition of helix-breaking solvent such as DMSO are then investigated to confirm such a structural model. Figure 4 shows cyclic voltammograms of **3** assembly covered electrode before and after treatment of DMSO.

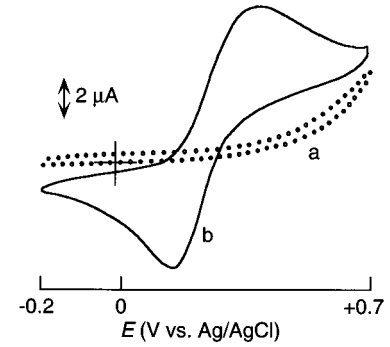

Figure 4. Typical change in cyclic voltammogram of **3**-monolayer-covered electrode by treating with DMSO: (a) as prepared from $CHCl_3$ solution; (b) as treated with DMSO. Experimental conditions are the same in Figure 3.

Table 1. Frequency Changes of QCM Electrode Due to Treatment of 3-Monolayer with DMSO

treatment	ΔF (Hz)	$\Delta m \times 10^7$ (g/cm^2)	A^a (nm^2/molecule)
as prepared	-44 ± 1	2.3 ± 0.1	2.9 ± 0.1
as treated with DMSO	-23 ± 2	1.3 ± 0.12	5.5 ± 0.1

[a] A = apparent occupied areas of **3** on gold surface.

Considerable decrease in the blocking ability toward $[Fe(CN)_6]^{4-}$ is observed after treatment of DMSO, indicating that the packing density of the SAM became loose. The QCM data for **3** assembly after treatment of DMSO are summarized in Table 1. It can be seen that the values of Δm and apparent occupied area per molecule became about $^1/_2$- and 2-fold, respectively, of those before treatment. This means that half of the molecules were released from the original assembly; i.e., they had not directly attached to the gold surface. One of the possible explanations for this phenomenon is as follows. The **3** molecule takes α-helix conformation and exists mainly in a dimeric form due to helix−helix interaction in $CHCl_3$, and the resultant assembly on gold surface must be in a double-layered structure. If this structural model would be resulted from a macrodipole interaction working between helices, the double-layered structure might be converted into the monolayer structure by weakening such a macrodipole interaction. The QCM data listed in Table 1 strongly support these considerations. The monolayer of **3** thus obtained would carry homogeneously distributed molecular cavities that must be suitable size for welcoming a guest helical PBLG.

Immobilization of Anthracene-Terminated PBLG through Helix−Helix Interaction on Gold. The interaction of helical guest PBLG **1** with the monolayer of **3** was examined in view of blocking ability toward $[Fe(CN)_6]^{4-}$ and the mass increase on gold surface. Figure 5A shows a change in the peak current of $[Fe(CN)_6]^{4-}$ by immersing the **3**-monolayer-covered electrode into a $CHCl_3$ solution containing **1**, and Figure 5B shows the resonance frequency change of quartz crystal upon addition of **1** under the same conditions for the electrochemical measurement.

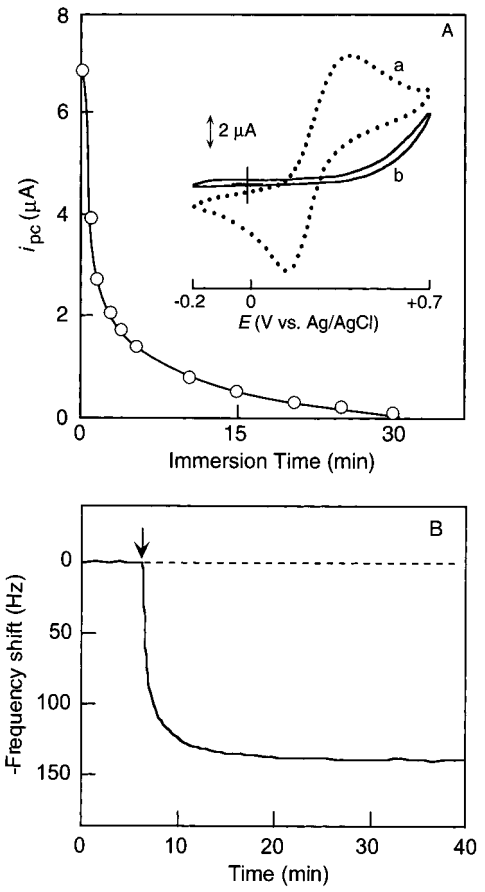

Figure 5. (A) Change in the peak current (i_p) of $[Fe(CN)_6]^{4-}$ due to incorporation of **1** into porous **3**-monolayer on gold electrode. Inset shows the typical change in cyclic voltammogram by immersing porous **3**-monolayer covered electrode into $CHCl_3$ solution of **1**: (a) 0 min and (b) 30 min immersion. Experimental conditions are the same in Figure 3. (B) Frequency shift of porous **3**-monolayer-covered QCM by addition of $CHCl_3$ solution of **1**. Experimental conditions are the same in Figure 4. Arrow indicates the addition of **1**.

The peak current of $[Fe(CN)_6]^{4-}$ steeply decreases with immersion because of incorporation of the guest **1** into the host **3**-monolayer on gold. The complexation of the guest **1** with **3**-monolayer is found to be completed after 30 min immersion, which leads the perfect blocking toward $[Fe(CN)_6]$.$^{4-}$ The result is also supported by QCM data as shown in Figure 5B. The resonance frequency decreases drastically with addition of the guest **1** and becomes unchanged after about 30 min at a frequency shift of -28 ± 2 Hz in dry air. Such a frequency decrease must be due to a mass increase on the QCM electrode, resulting from the adsorption of the guest **1** onto the **3**-monolayer. The total mass increase (Δm) could be calculated to be $(1.5 \pm 0.1) \times 10^{-7}$ g/cm^2. By using both this value and the values listed in Table 1, one can compute the molar ratio of the guest **1** molecule to **3** molecule of the host monolayer to be close to unity, implying the formation of a 1:1 complex through an interhelix interaction. If such an interaction is based upon the helix−macrodipole moment and allows antiparallel orientation of helical rods, the anthryl group of **1** is expected to be fixed at the monolyer surface, and then the DNA duplex must be bound to the monolayer surface through the intercalation of anthryl groups. Consequently, a novel DNA−polypeptide hybridized ultrathin film would be constructed on a gold surface. A reference compound of **2**, which has no anthryl group at the terminal end of PBLG segment but has the same segment length with that for **1**, was incorporated into the host **3**-monolayer on gold in the same manner as described above. The formation of a 1:1 complex between the guest **2** and the **3**-monolayer was also observed. In addition, the ternary monolayers composed of **1**, **2**, and **3** were prepared by mixing of **1** and **2** in $CHCl_3$ solution at various compositions (f_1: molar fraction of **1)** and then incorporated into the **3**-monolayers. First, to obtain information about the orientational state of helical PBLG rods on gold surface, reflection−absorption (RA) FTIR spectra were measured. Enriquez et al. demonstrated that the nature of the order and average orientation of the polypeptide α-helix in the films can be inferred from RA-FTIR data.[34,35] In the amide I and amide II regions (1700−1500 cm^{-1}), all spectra of **3**-monolayer before and after treatment with DMSO, and mixed monolayer composed of **1**, **2**, and **3** prepared at $f_1 = 0.3$ exhibit two bands at 1660 and 1550 cm^{-1}, which are assigned to the α-helix structure.[33] The additional C=O stretching band due to ester groups of the side chain of PBLG is observed at 1740 cm^{-1}. By using the ratio of the integrated intensities of the amide I and amide II regions, the average tilt of the helix axis from the surface normal was evaluated to be $43 \pm 3°$ for the **3**-monolayer as prepared from $CHCl_3$ and $66 \pm 3°$ for **3**-monolayer after treatment with DMSO and then with $CHCl_3$ (Chart 1). Such a difference in the tilting angle can be reasonably interpreted by accounting for the molecular packing density and interhelix interaction in the monolayers. The rigid PBLG helical rods, anchored to the gold surface through a flexible methylene spacer, will lie as flat as possible on the substrate. However, for the densely packed **3**-monolayer as prepared from $CHCl_3$, in which the helical rods are aligned in the antiparallel manner based on the attractive interaction between macrodipoles, the helices are obliged to orient more perpendicularly to the surface due to crowding with the helical rods. On the other hand, the porous **3**-monolayer, in which the helical rods are loosely packed and aligned in the parallel manner, horizontal orientation of helices to the surface must be favored because of an energetically unfavorable parallel packing of the macrodipoles and a release of the crowding with helical rods in the monolayer. The tilting angle of the helical rods for mixed monolayer composed of **1**, **2**, and **3** ($f_1 = 0.3$) reverted to that ($43 \pm 3°$) of the original double-layered **3**-assembly (Chart 1).

DNA Binding Properties of Anthryl Groups-Tagged PBLG Film on Gold Surface. The interaction of the **2**/**3** binary monolayer with DNA was tested for comparison with the monolayer containing **1**. When the resonance frequency became unchanged within ± 1 Hz in 5 mM Tris/HCl buffer at pH 7.2, in which the **2**/**3** binary monolayer-deposited QCM resonator was placed, a buffer solution of DNA was injected, and the frequency shift was recorded as shown in Figure 6a.

Upon addition of DNA solution, the frequency decrease is observed by a slight shift, and the same tendency of frequency shift is also observed in the blank experiment, in which the buffer solution without DNA was added. Therefore, the observed small shift must be due to some physical changes around the QCM electrode by addition of aqueous solutions. In fact, when the resonance frequency was measured in dry air, no frequency difference was observed within experimental

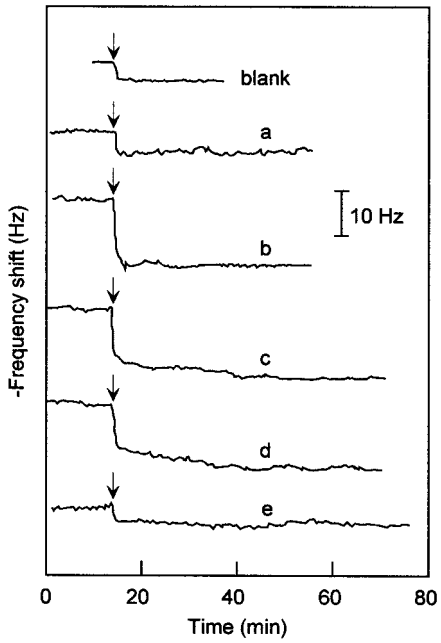

Figure 6. Frequency shifts of **1**, **2**, and **3**-mixed monolayers covered QCMs prepared from $f_1 = 0$ (a), 0.3 (b), 0.5 (c), 0.6 (d), and 1.0 (e) upon addition of DNA solution at pH 7.2 ([DNA-(phosphate unit)] = 1.0×10^{-5} M.

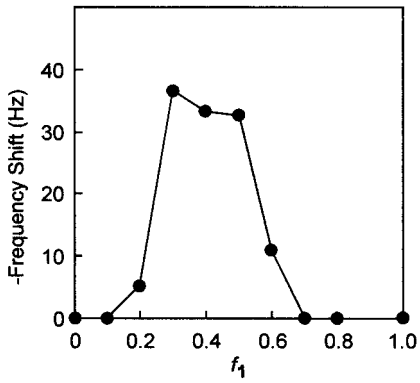

Figure 7. Frequency shift due to adsorption of DNA onto **1**, **2**, and **3**-mixed monolayers covered QCMs as a function of f_1.

errors before and after addition of DNA solution. These results suggest that this binary monolayer did not bind DNA duplex. On the other hand, for the monolayers composed of **1**, **2**, and **3**, which were prepared by mixing **1** and **2** in $CHCl_3$ solution at various compositions (f_1 = 0.3, 0.5, 0.6, and 1.0) and then incorporated into the **3**-monolayers (Figure 6b−e), obvious frequency decreases were observed, suggesting binding of DNA onto mixed monolayer surfaces. The same experiment was performed for the monolayers prepared from the other compositions of f_1. Figure 7 shows a total frequency shift during adsorption of DNA as a function of the f_1 value.

It is clearly seen from the figure that the amount of the frequency shift depends on the monolayer composition, f_1, and the mixed monolayers prepared at higher f_1 values (f_1 = 0.7−1.0) do not allow to interact with DNA. This result suggests that the lateral density of the anthryl group on the monolayer surface is too high to intercalate with DNA. In the lower f_1 region (f_1 < 0.7), however, more effective binding of DNA is found to take place, indicating the necessity to avoid the steric crowdedness for optimized binding capacity. To confirm the immobilization of DNA onto the mixed monolayer

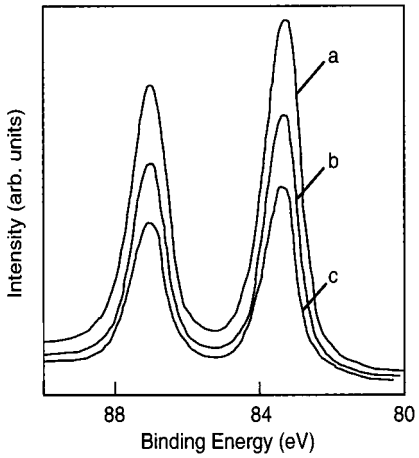

Figure 8. XPS Au_{4f} spectra at a 90° takeoff angle for a bare substrate (a) **1**, **2**, and **3**-mixed monolayer prepared at f_1 = 0.3 (b) and after immersing this monolayer into DNA solution (c).

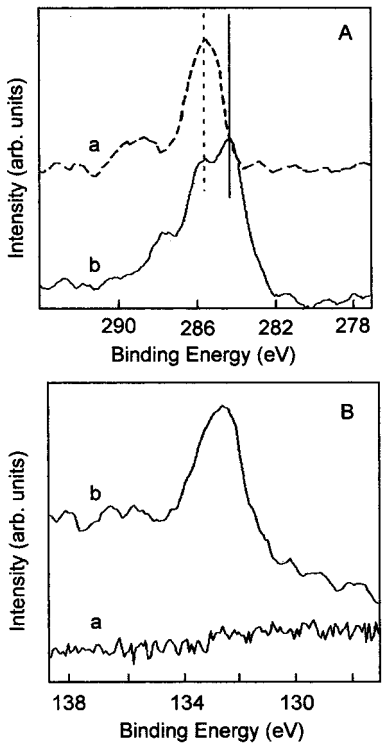

Figure 9. XPS C 1s (A) and P 2p (B) spectra at a 90° takeoff angle for **1**, **2**, and **3**-mixed monolayer prepared at f_1 = 0.3 (a) and after immersing this monolayer into DNA solution (b).

(f_1 = 0.3), XPS spectra were measured before and after binding of DNA duplex (Figure 8).

Attenuation of the gold signal for the monolayer after immersing into a DNA solution is observed, resulting from the immobilization of DNA onto the monolayer surface. Additionally, the film thickness could be estimated from XPS data based on the exponential attenuation of the Au 4f signal,[36] wherein the mean free path of Au photoelectron through an organic overlayer was obtained using a monolayer of hexadecanethiol as a standard.[37] For the monolayers (f_1 = 0.3) before and after binding of DNA, the film thicknesses were evaluated to be 2.0 and 3.6 nm, respectively, were obtained; i.e., the average thickness of DNA overlayer can be calculated to be 1.6 nm. This value may be reasonable and demonstrates that the DNA overlayer must not be

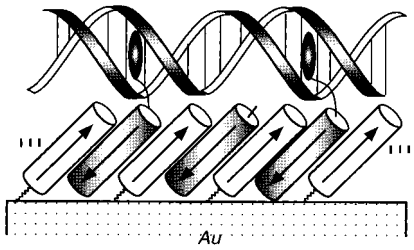

Figure 10. Possible illustration of DNA−PBLG hybridized thin film on gold surface.

at least a multilayer structure, since the diameter of DNA is known to be about 2 nm although it is sensitive to its surroundings. Further direct evidence of immobilization of DNA onto the monolayer surface was obtained by P_{2p} and C_{1s} signals as shown in Figure 9.

In the P_{2p} region, the signal at 133 eV assigned to the phosphate unit of DNA was observed, which was not appeared at all in the spectrum before binding. In the C_{1s} region, the characteristic signal of DNA assigned to the nucleic acid base is observed at 284 eV besides the other contributions. Therefore, it is evident that the successful binding of DNA is performed at the two-dimensional polypeptide monolayer surface as illustrated schematically in Figure 10.

Orientational variation of PBLG helical rods on gold surface induced by hybridization with DNA was further tried to examine by measuring the RA-FTIR spectrum. The O=P−O− stretching vibration assigned to the phosphate unit of DNA was clearly observed at 1060 cm^{-1} in addition to the C=O, C=C, and C=N vibration assigned to the nucleic acid base at 1700−1500 cm^{-1}. The amide I and amide II bands of PBLG segment were unfortunately superposed by remarkable absorptions of nucleic acid base, and it was therefore difficult to examine the change in the orientation of PBLG helical rods on gold surface.

Conclusions

We have demonstrated a novel approach for organization of functional groups such as DNA intercalator, anthracene, by a host−guest helix−macrodipole interaction and a specific interaction with DNA. The SAM film of **3** prepared from the $CHCl_3$ solution would take a double-layered structure consisting of the dimeric aggregate of helices. When the helix-breaking solvent such as DMSO was added to the solution, the SAM film of **3** could provide homogeneously distributed molecular cavities within the film. The porous monolayer thus obtained could uptake the guest PBLG helices carrying an anthryl group at the C-terminal end, allowing the anthryl groups oriented to the solution phase due to antiparallel macrodipole interaction. Effective binding of DNA was accomplished when the surface density of anthryl group was controlled to be appropriate. The study on the electron transfer through oriented DNA−helical polypeptide film on gold electrode is now in progress.

Acknowledgment. This work was supported in part by the project "Nano Structure Hybrid" of High Technology Center at RCAST of Doshisha University.

References and Notes

(1) Whitesell, J. K.; Chang, H. K. *Science* **1993**, *621*, 73.
(2) Worley, C. G.; Linton, R. W.; Samulski, E. T. *Langmuir* **1995**, *11*, 3805.
(3) Miura, Y.; Kimura, S.; Imanishi, Y.; Umemura, J. *Langmuir* **1998**, *14*, 2761.
(4) Fujita, K.; Bunjes, N.; Nakajima, K.; Hara, M.; Sasabe, H.; Knoll, W. *Langmuir* **1998**, *14*, 6167.
(5) Higashi, N.; Shimoguchi, M.; Niwa, M. *Langmuir* **1992**, *8*, 1509.
(6) Higashi, N.; Sunada, M.; Niwa, M. *Langmuir* **1995**, *11*, 1864.
(7) Niwa, M.; Matsui, M.; Koide, K.; Higashi, N. *J. Mater. Chem.* **1997**, *7*, 2191.
(8) Niwa, M.; Morikawa, M.; Higashi, N. *Langmuir* **1999**, *15*, 5088.
(9) Niwa, M.; Morikawa, M.; Higashi, N. *Angew. Chem., Int. Ed.* **2000**, *39*, 960.
(10) Niwa, M.; Murata, T.; Kitamatsu, M.; Matsumoto, T.; Higashi, N. *J. Mater. Chem.* **1999**, *9*, 343.
(11) Nuzzo, R. G.; Allara, D. L. *J. Am. Chem. Soc.* **1983**, *105*, 4481.
(12) Katz, E.; Willner, I. *Langmuir* **1997**, *13*, 3364.
(13) Frey, B. L.; Jordan, M.; Schmitt, F.-J.; Guder, H.-J.; Angermaier, L.; Knoll, W. *J. Chem. Phys.* **1993**, *99*, 7012.
(14) Niwa, M.; Mori, T.; Higashi, N. *Macromolecules* **1993**, *26*, 1936.
(15) Spinke, J.; Liley, C. E.; Kornguth, S.; Corn, R. M. *Anal. Chem.* **1995**, *67*, 4452.
(16) Willner, I.; Lapidot, N.; Riklin, A.; Kasher, R.; Zahavy, E.; Katz, E. *J. Am. Chem. Soc.* **1994**, *66*, 1535.
(17) Kumar, A.; Biebuyck, H. A.; Whitesides, G. M. *Langmuir* **1994**, *10*, 1498.
(18) Zhong, C.-J.; Porter, M. D. *Anal. Chem.* **1995**, *67*, 709A.
(19) Higashi, N.; Inoue, T.; Niwa, M. *Chem. Commun.* **1997**, 1507.
(20) Higashi, N.; Takahashi, M.; Niwa, M. *Langmuir* **1999**, *15*, 111.
(21) Okahata, Y.; Kobayashi, T.; Tanaka, K.; Shimomura, M. *J. Am. Chem. Soc.* **1998**, *120*, 6165.
(22) Arkin, M. R.; Stemp, E. D. A.; Holmlin, R. E.; Barton, J. K.; Hormann, A.; Olson, E. J. C.; Barbara, P. F. *Science* **1996**, *273*, 475.
(23) Kelley, S. O.; Jackson, N. M.; Hill, M. G.; Barton, J. K. *Angew. Chem., Int. Ed.* **1999**, *38*, 941.
(24) Wada, A. *Adv. Biophys.* **1976**, *9*, 1.
(25) Hol, W. G. J.; van Duijnen, P. T.; Berendsen, H. J. C. *Nature (London)* **1978**, *273*, 443.
(26) Porumb, H. *Prog. Biophys. Mol. Biol.* **1978**, *34*, 175.
(27) Fukuda, R.; Takenaka, S.; Takagi, M. *J. Chem. Soc., Chem. Commun.* **1990**, 1028.
(28) Asakawa, M.; Endo, K.; Kobayashi, K.; Toi, H.; Aoyama, Y. *Bull. Chem. Soc. Jpn.* **1992**, *65*, 2050.
(29) Tomosaka, H.; Omata, S.; Anzai, K. *Biosci. Biotechnol. Biochem.* **1994**, *58*, 1420.
(30) Niwa, M.; Mori, T.; Nishio, E.; Nishimura, H.; Higashi, N. *J. Chem. Soc., Chem. Commun.* **1992**, 547.
(31) Sauerbrey, G. *Z. Phys.* **1959**, *155*, 206.
(32) Chang, Y.-C.; Frank, C. W. *Langmuir* **1996**, *12*, 5824.
(33) Miyazawa, T.; Blout, E. R. *J. Am. Chem. Soc.* **1961**, *83*, 712.
(34) Tsuboi, M. *J. Polym. Sci.* **1962**, *59*, 139.
(35) Enriquez, E. P.; Samulski, E. T. *Mater. Res. Soc. Symp. Proc.* **1992**, *255*, 423.
(36) Pressprich, K. A.; Maybury, S. G.; Thomas, R. E.; Linton, R. W.; Irene, E. A.; Murray, R. W. *J. Phys. Chem.* **1989**, *93*, 5568.
(37) Bain, C. D.; Troughton, E. B.; Tao, Y.-T.; Evall, J.; Whitesides, G. M.; Nuzzo, R. G. *J. Am. Chem. Soc.* **1989**, *111*, 321.

MA0116093